Происхождение космических лучей с энергиями от 10^6 до 10^{21} эВ

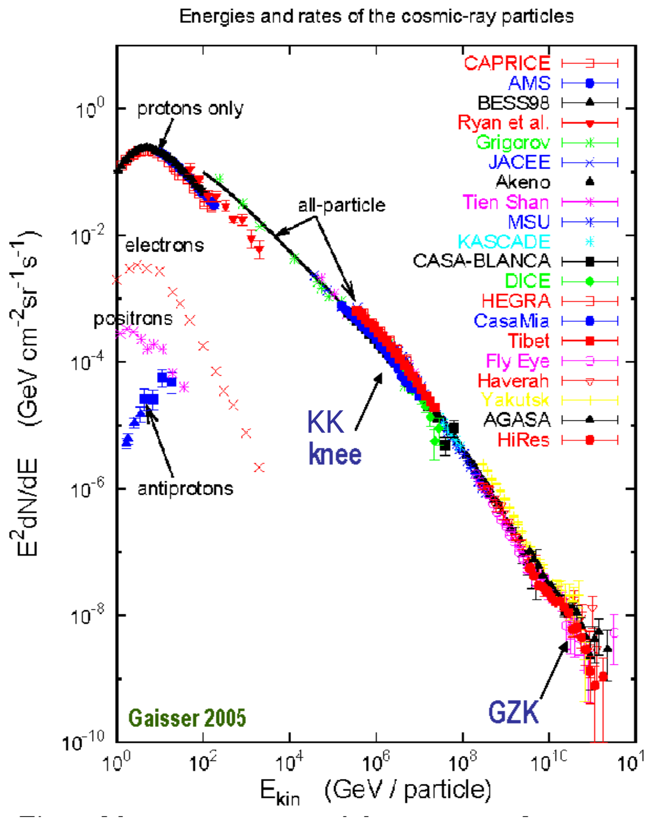

В.С. Птускин

ИЗМИРАН

Дубна 2014

Voyager 1 at the edge of interstellar space

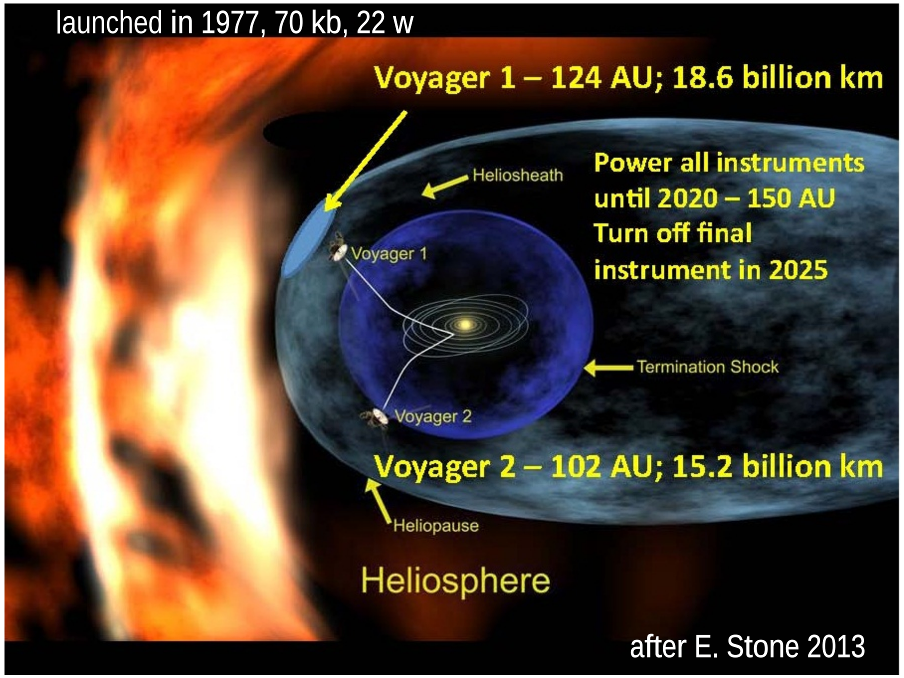

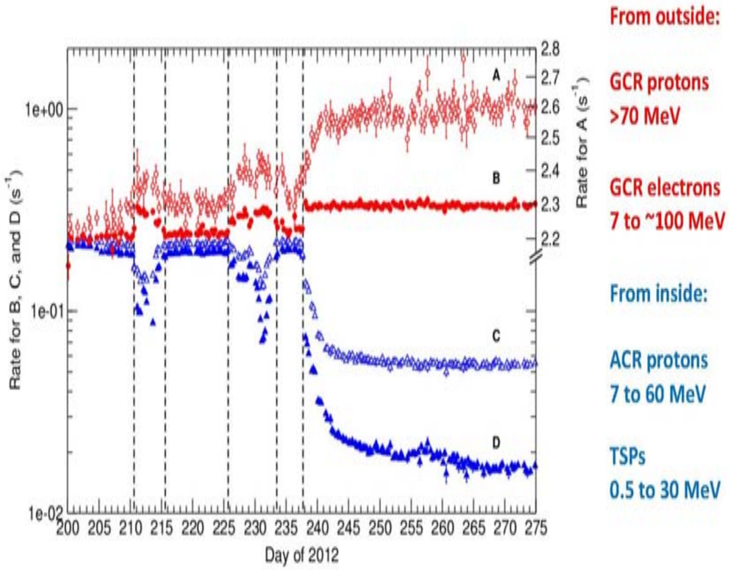

direct measurements of interstellar CR spectra at low energies

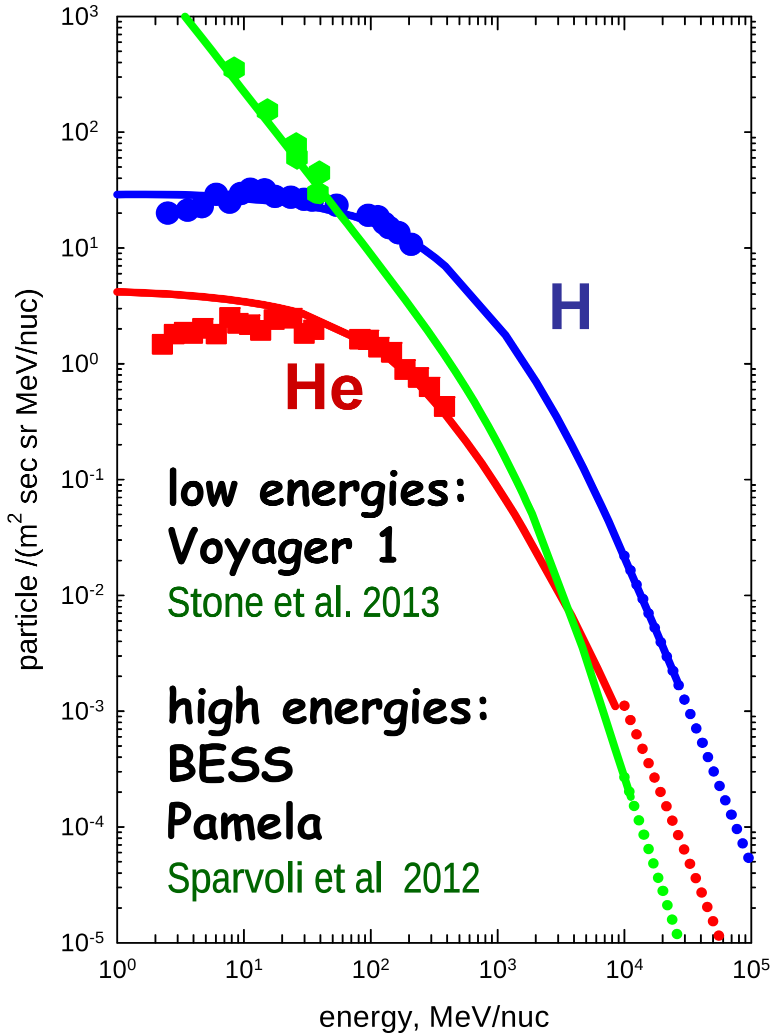

poster VP, Seo, Zirakashvili

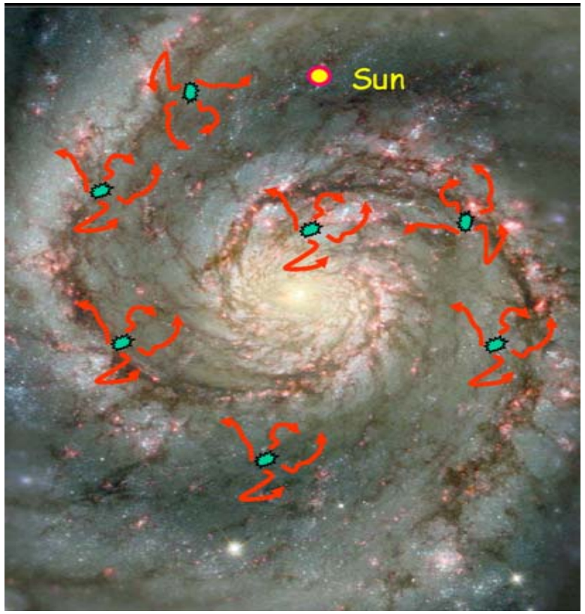

energy balance: ~ **15%** of SN kinetic energy go to cosmic rays to maintain cosmic ray density   Ginzburg & Syrovatsky 1963

steady state (without energy loss):

$$J_{cr}(E)= Q_{cr}(E)\times T_e(E)$$

source, $E^{-2.2}$

escape time from the Galaxy, $E^{-0.5}$
~ 10^8 yr at 1 GeV;
cosmic-ray halo H = 4 kpc

propagation: diffusion in galactic magnetic fields, resonant scattering $k_{res} \sim 1/r_g$, $D \sim 3\times10^{28}$ cm^2/s, 1 GeV/n, escape length $X_e = v\langle\rho\rangle T_e = v\mu H/2D \sim 10$ g/cm^2 from B/C ratio

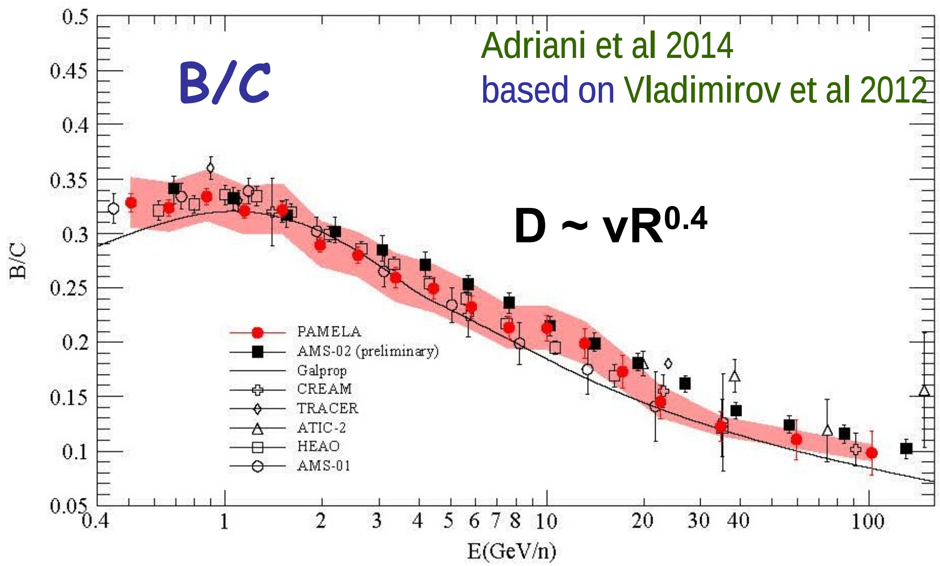

galactic wind driven by cosmic rays

Ipavich 1975, Breitschwerdt et al. 1991, 1993

u_{inf} = 500km/s R_{sh} = 300 kpc

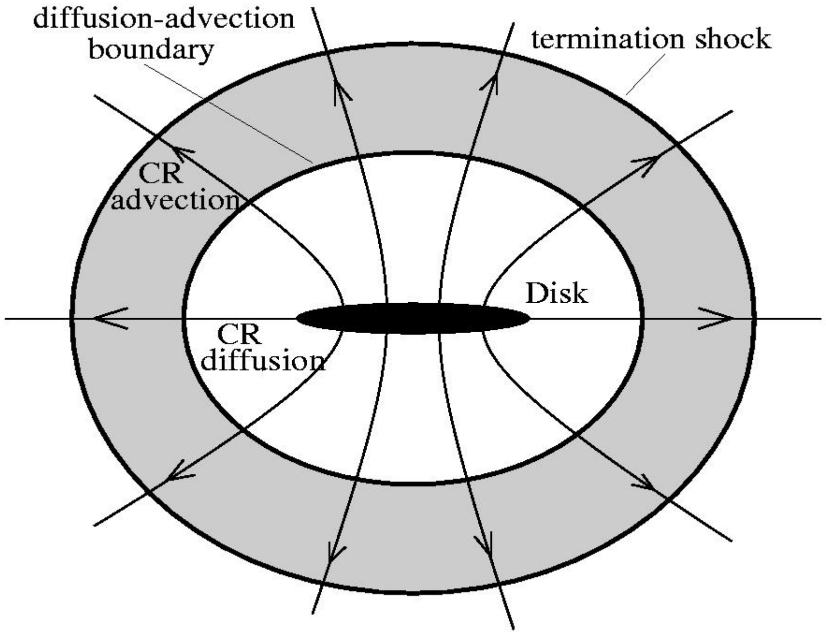

CR scale height is larger then the scale height of thermal gas. CR pressure gradient drives the wind.

+ **cosmic ray streaming instability with nonlinear saturation**

Zirakashvili et al. 1996, 2002, 2005, VP et al. 1997, 2000,

$$D \sim \frac{\mathrm{v}B}{q_{cr}}\left(\frac{p}{Zm_pc}\right)^{\gamma_s - 1} \approx 10^{27}\beta\left(\frac{p}{Zm_pc}\right)^{1.1} \mathrm{cm}^2/s,$$

$$\gamma = (3\gamma_s - 1)/2 \approx 2.7, \quad \text{at} \quad \gamma_s \approx 2.1$$

$$X \sim \frac{H_{ef}}{D} \sim \left(\frac{p}{Zm_pc}\right)^{\frac{\gamma_s - 1}{2}} \sim \left(\frac{p}{Z}\right)^{-0.55}$$

diffusive shock acceleration

Fermi 1949, Krymsky 1977, Bell 1978, ...

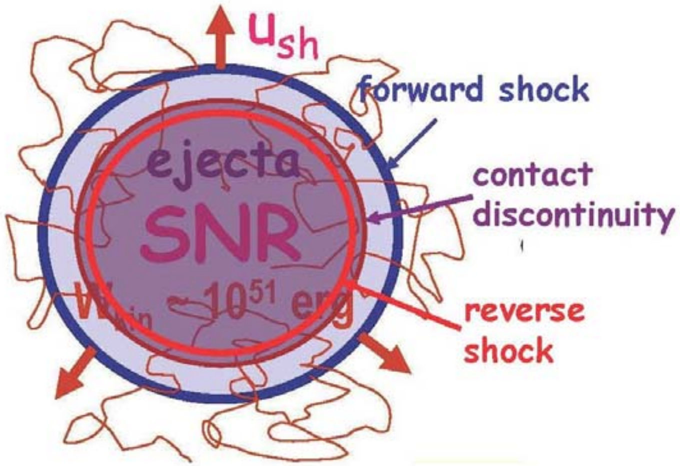

$$J \sim p^{-\gamma_s}, \quad \gamma_s = \frac{\sigma + 2}{\sigma - 1} = 2$$

for test particles !

compression ratio = 4

$$\boxed{\frac{u_{sh} R_{sh}}{D(p)} > 10}$$

-condition of CR acceleration and confinement

- D(p) should be anomalously small both upstream and downstream; CR streaming creates turbulence in shock precursor

Bell 1978; Lagage & Cesarsky 1983; McKenzie & Vőlk 1982 ...

"Bohm" limit $D_B = v r_g/3$: $E_{max} \approx 0.3 \cdot Ze \cdot \frac{u_{sh}}{c} \cdot B \cdot R_{sh}$

$\boxed{E_{max,ism} = 10^{13} \ldots 10^{14}\, Z\ \mathrm{eV}}$ for $B_{ism} = 5\ 10^{-6}$ G

$\sim B_{sh} t^{-1/5}$ at Sedov stage

abandonment of interstellar Bohm limit hypotheses;

$D \not\approx D_{B,ism}$

SN 1006

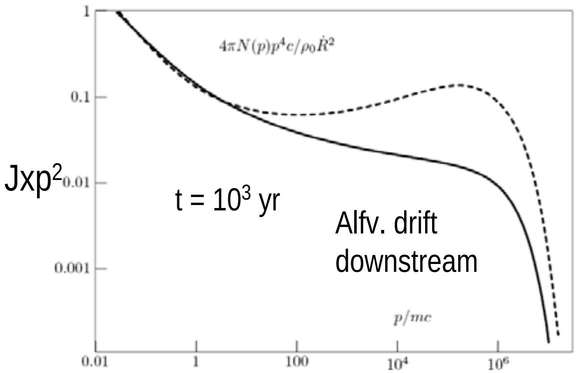

- strong cosmic-ray streaming instability gives

$\delta B >> B_{ism}$ in young SNR Bell & Lucek 2000, Bell 2004

Pelletier et al 2006; Amato & Blasi 2006; VZ & VP 2008; Vladimirov et al 2009; Gargate & Spitkovsky 2011

under extreme conditions (SN Ib/c, e.g. SN1998 bw)

$E_{max} \sim 10^{17} Z\,(u_{sh}/3\times10^4\ \mathrm{km/s})^2\, M_{ej}^{1/3} n^{1/6}$ eV

$B_{max} \sim 10^{-3}\,(u_{sh}/3\times10^4\ \mathrm{km/s})\, n^{1/2}$ G

confirmed by X-ray observations of young SNRs

SN 1006, Cas A, Tycho, RCW 86, Kepler, RX J1713.7-3946, Vela Jr., G1.9+0.3

$B^2/8\pi = 0.035\ \rho u^2/2$ Voelk et al. 2005

- wave dissipation in shock precursor leads to rapid decrease of δB and E_{max} with time

VP & VZ 2003

- finate V_a leads to steeper CR spectrum

$$\sigma = \frac{u_1 - V_{a,1}}{u_2 + V_{a,2}}$$

$$P_{cr} = \xi_{cr} \rho u_{sh}^2, \;\; \xi_{cr} \sim 0.5$$

- back reaction of cosmic-ray pressure modifies the shock and produces concave particle spectrum

Axford 1977, 1981; Eichler 1984; Berezhko et al. 1996, Malkov et al. 2000; Blasi 2005

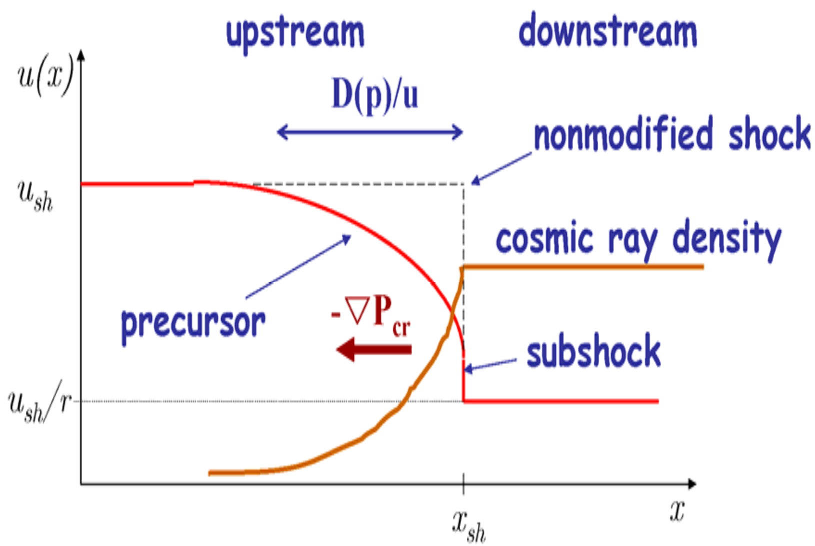

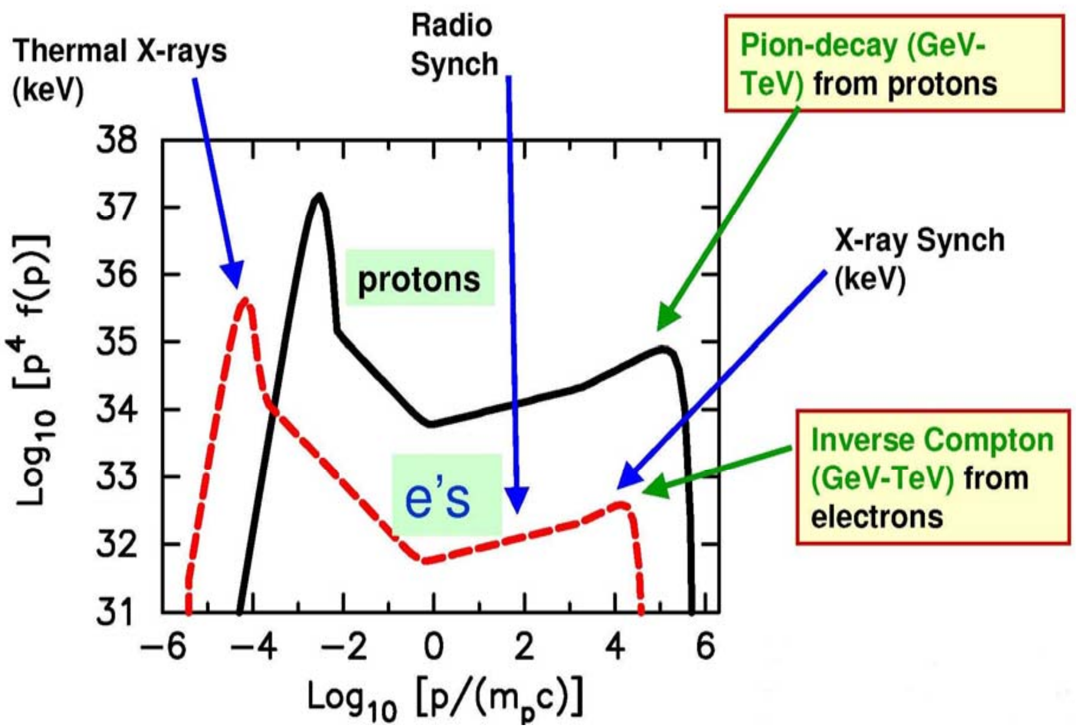

after Ellison

numerical simulations of particle acceleration and radiation in SNR

Berezhko et al. 1994-2006, Kang & Jones 2006
Zirakashvili & VP 2012,
semianalytic models Blasi et al.(2005), Ellison et al. (2010))

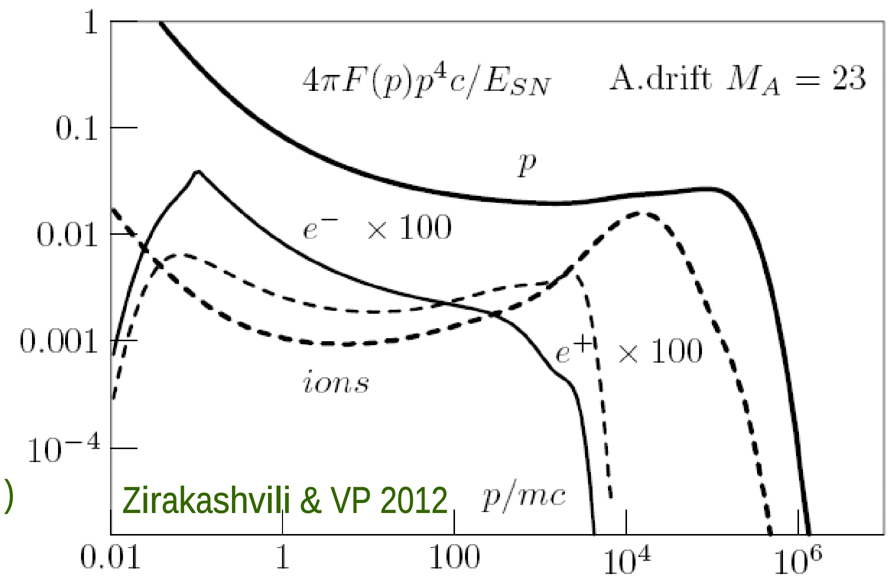

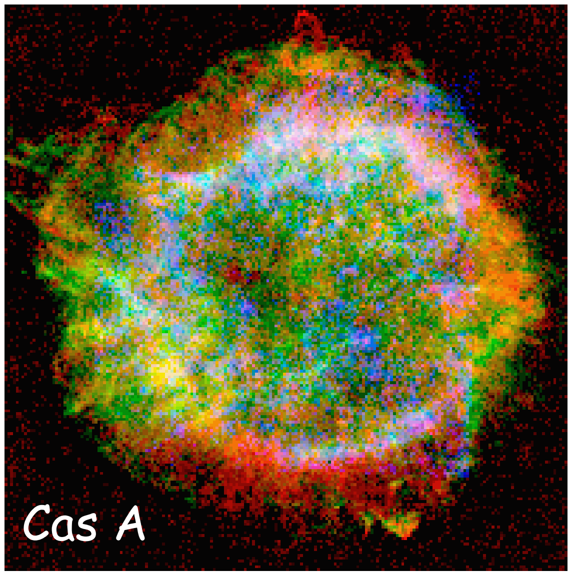

radio polarization in red (VLA),
X-rays in green (CHANDRA),
optical in blue (HST)

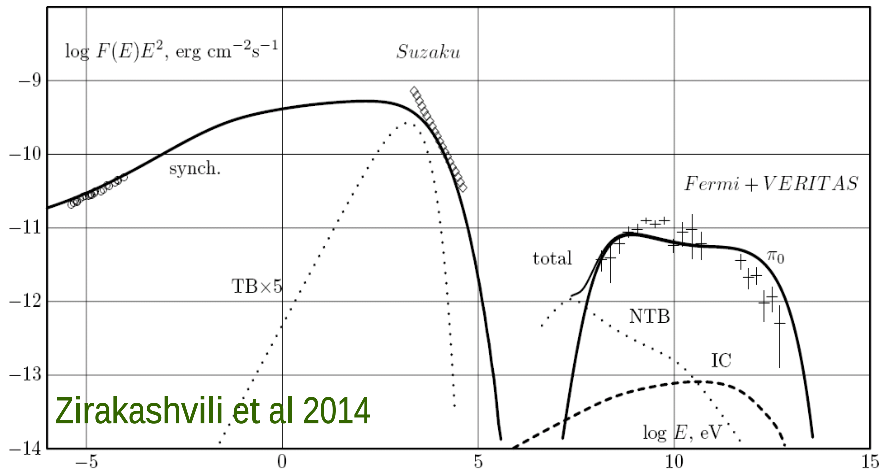

Fig. 6.— The broad-band spectral energy distribution of nonthermal radiation of Cas A calculated within the hadronic model H1. The following radiation processes are taken into account: synchrotron radiation of accelerated electrons (solid curve on the left), IC emission (dashed line), gamma-ray emission from pion decay (solid line on the right), thermal bremsstrahlung (dotted line on the left), nonthermal bremsstrahlung (dotted line on the right). Experimental data in gamma-ray (Fermi LAT, present work); VERITAS, Acciari et al. 2010, data with error-bars) and radio-bands (Baars 1977, circles), as well as the power-law approximation of Suzaku X-ray data (Maeda et al. 2009, diamonds) from the whole remnant are also shown.

calculated spectrum of Galactic cosmic rays:

VP, Zirakashvili, Seo 2010

source spectra produced by SNRs

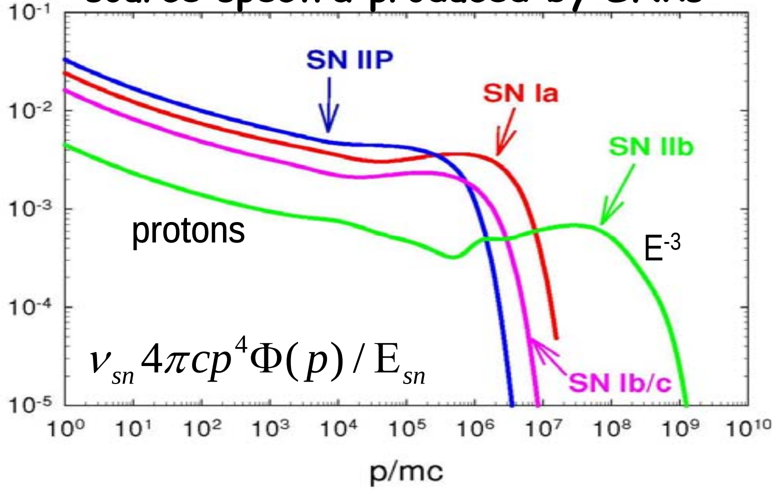

hydrodynamic eqs.+ P_{cr};
diffusion-convection
transport eq. for CR with
Alfvenic drift

«knee» is formed at
the beginning of Sedov stage

$$E_{knee}/Z = 1.1\times 10^{15}\, W_{sn,51} n^{1/6} M_{ej}^{-2/3}\ \text{eV}$$

$J\times E^{2.75}$

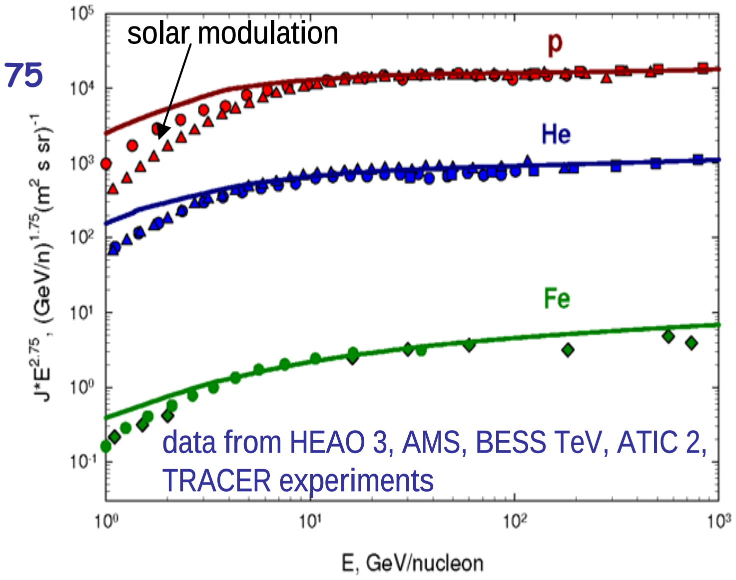

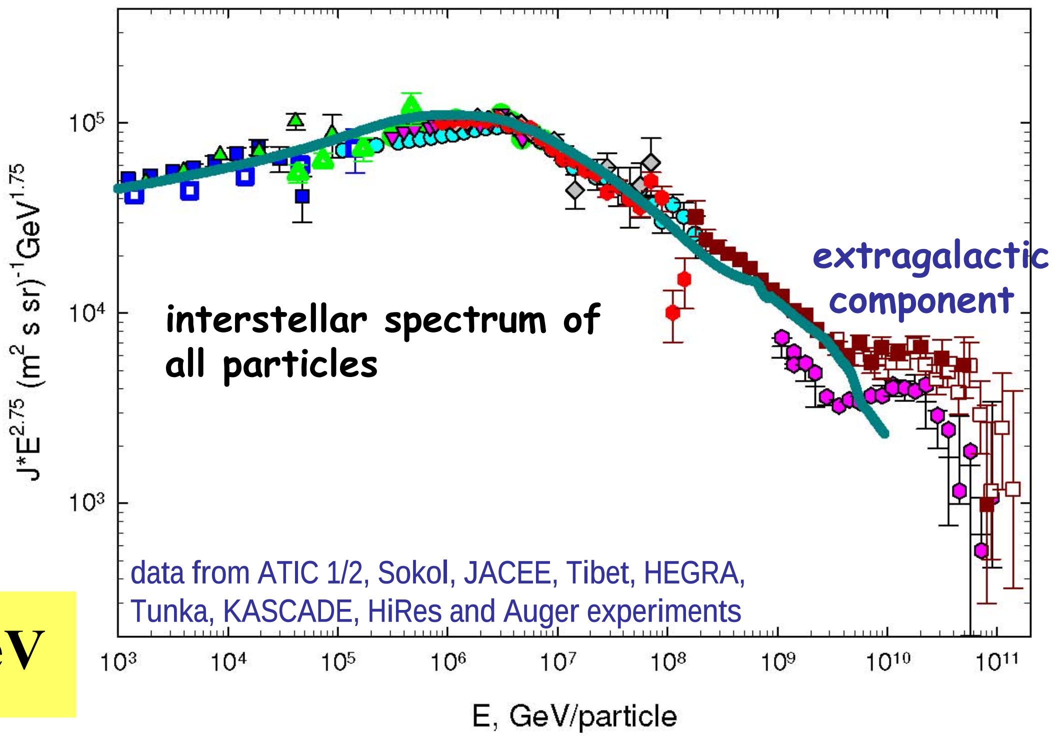

features to explain:

hardening above 200 GeV/nucleon

new source
Zatsepin & Sokolskaya 2006

reacceleration in local bubble
Erlykin & Wolfendale 2011

superposition of sources
Thoudam & Horandel 2013

spectra of p and He are different

shock goes through material enriched in He
Ohira & Ioka 2011

H and He injection are different
Malkov et al. 2011

testing different scenarios

Vladimirov et al 2011

both features are explained when reverse SNR shock acceleration is included

VP, Zirakashvili, Seo 2012

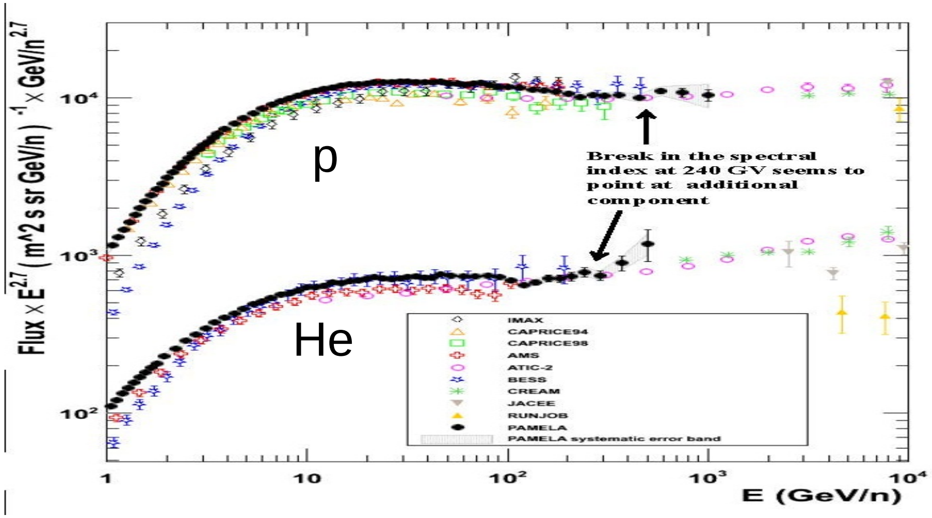

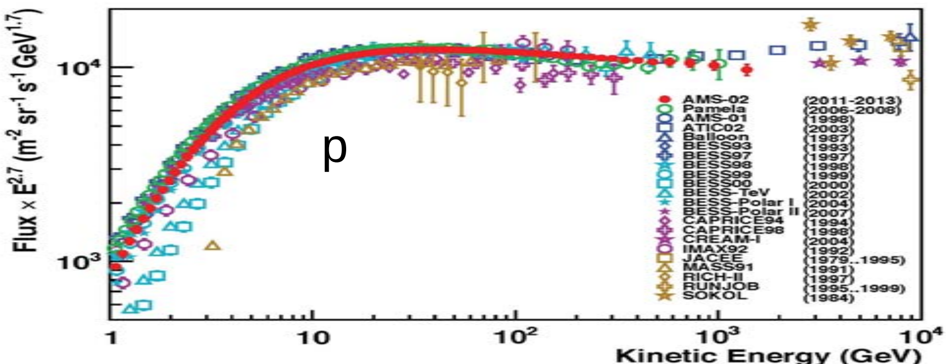

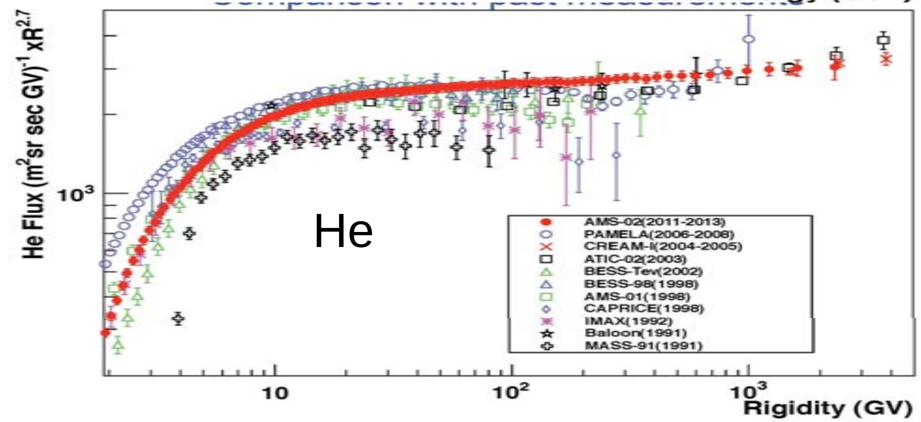

positrons in cosmic rays

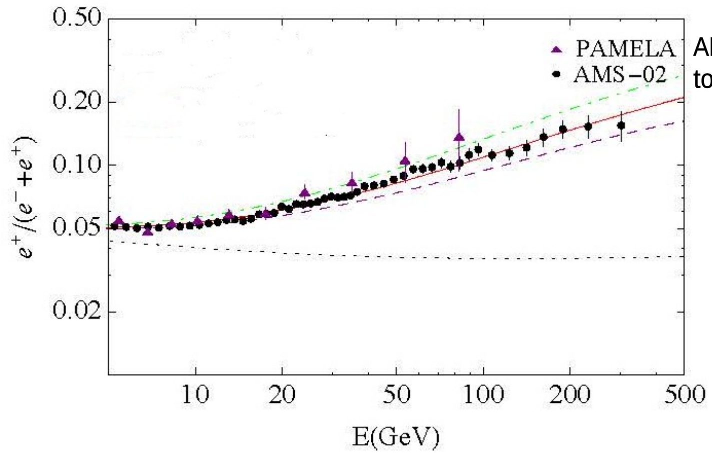

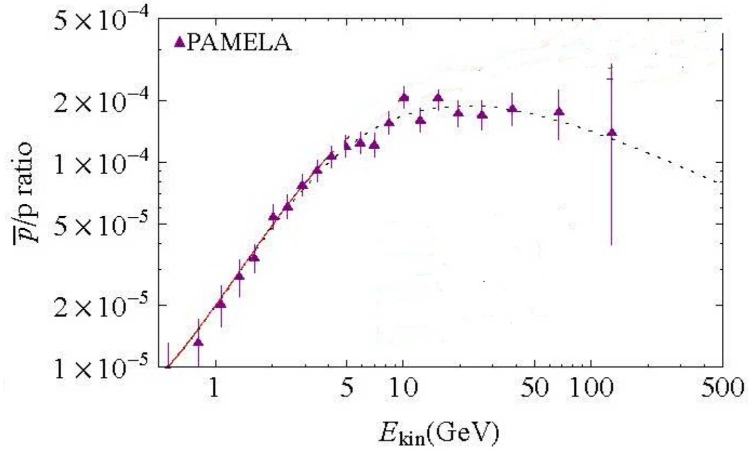

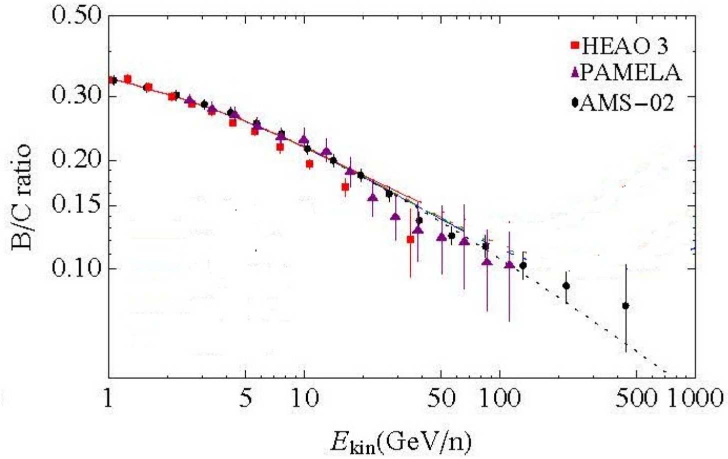

GALPROP calculations Cholis, Hooper 2014

H = 4 kpc

$D = 2.95\ 10^{28} v (R/3\ \mathrm{GV})^{0.43}\ \mathrm{cm^2/s}$

$V_a = 10$ km/s

pulasar origin Harding, Ramaty 1987, Aharonian et al. 1995, Hooper et al. 2008, Malyshev et al. 2009

e+ production and acceleration in shell SNRs Blasi 2009, Berezhko, Ksenofontov 2013

reverse shock in radioactive ejecta Ellison et al 1990, Zirakashvili, Aharonian 2011

annihilation and decay of dark matter Tylka 1989, Fan et al 2011

Отношения субжелезо/железо:
субжелезо - из ATIC.
железо - из TRACER и CREAM

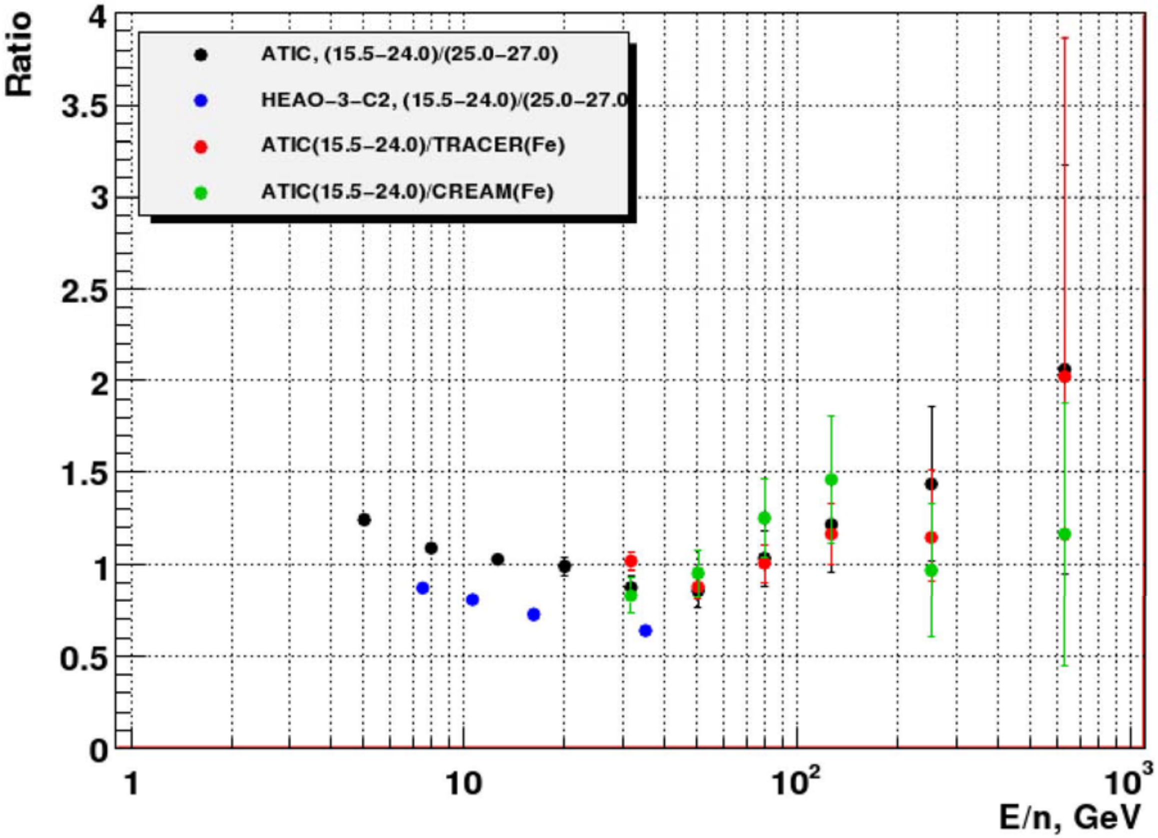

Zatsepin, Panov, Sokolskaya 2012

Prosin et al. 2014

knee and beyond

different types of nuclei,
$E_{knee} \sim Z$;
different types of SNRs;
transition to extragalactic CR

knee at 3-4 PeV
hardening at 20-30 PeV,
2nd knee at 200-300 PeV;
contribution of extragalactic
protons ~50% at ~ 200 PeV
Sveshnikova et al 2013

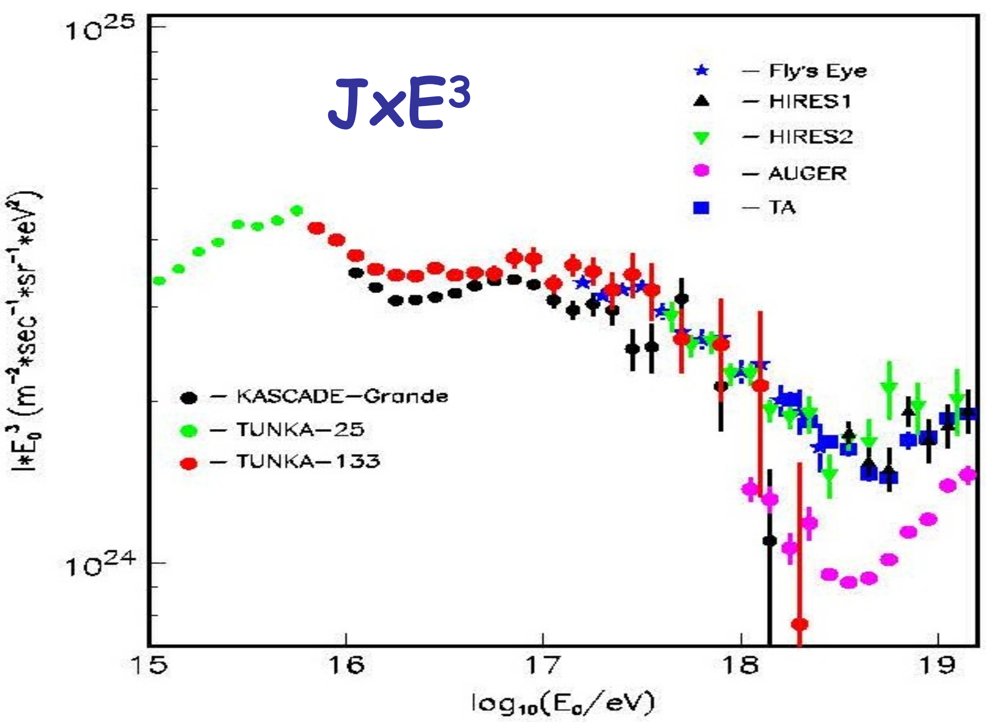

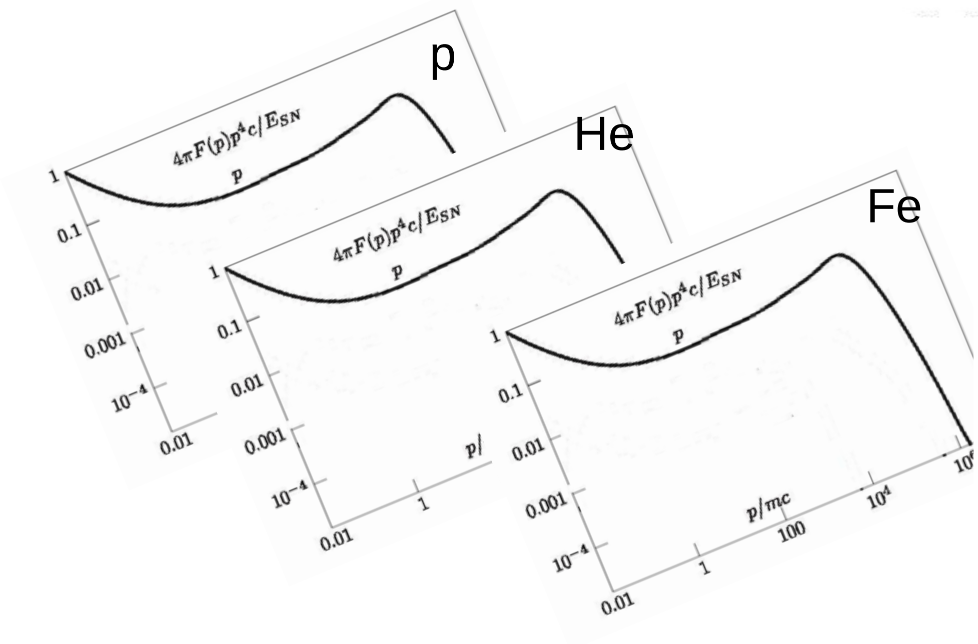

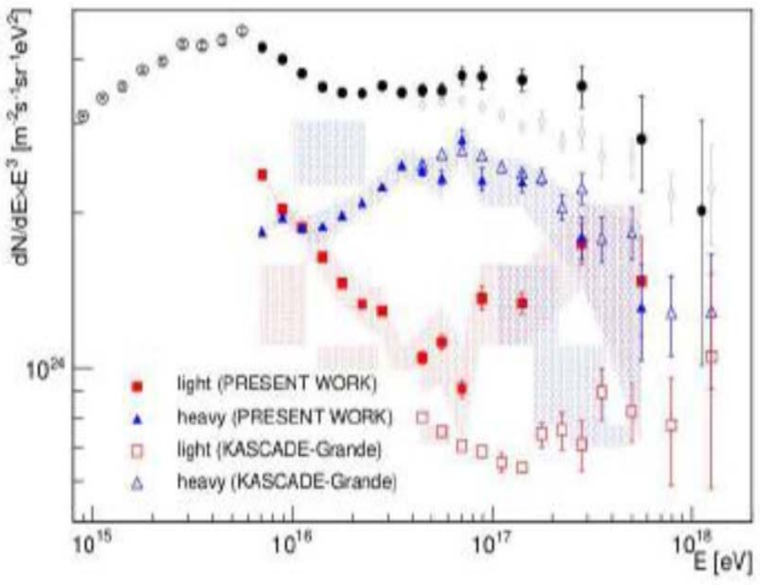

extension of Galactic propagation model up to $10^{19}Z$ eV: trajectory calculations

Syrovatsky 1971, Berezinsky et al. 1991, Gorchakov et al 1991, VP et al 1993, Lampard et al 1997, Zirakashvili et al 1998, **Hörandel et al. 2005**

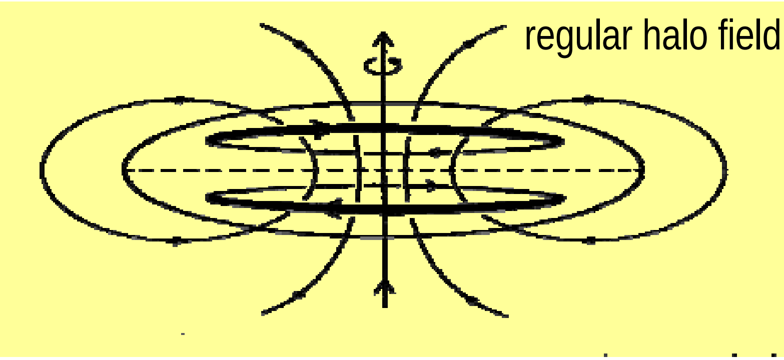

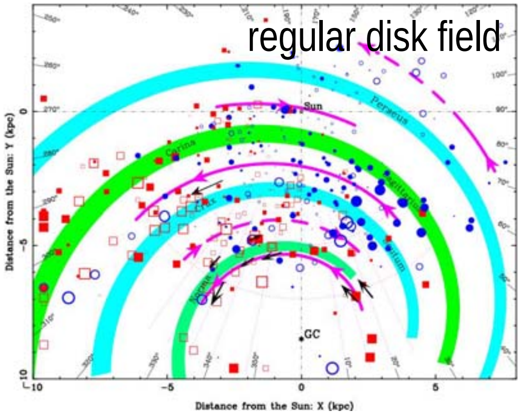

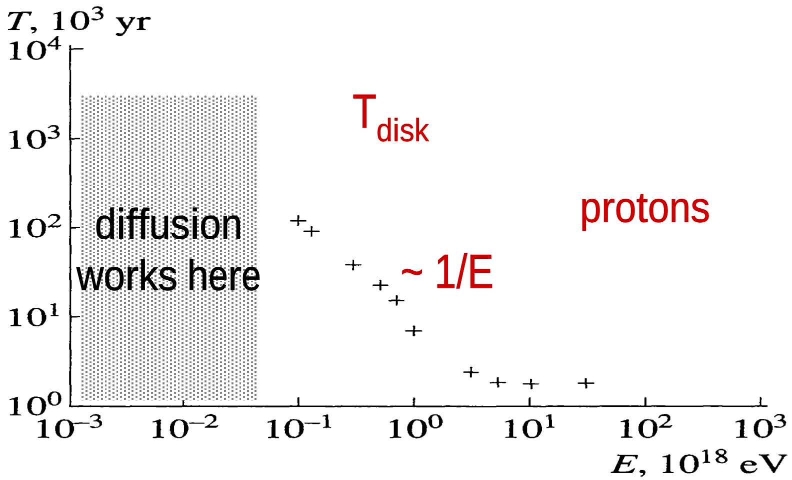

cosmic ray anisotropy, equatorial dipole amplitude

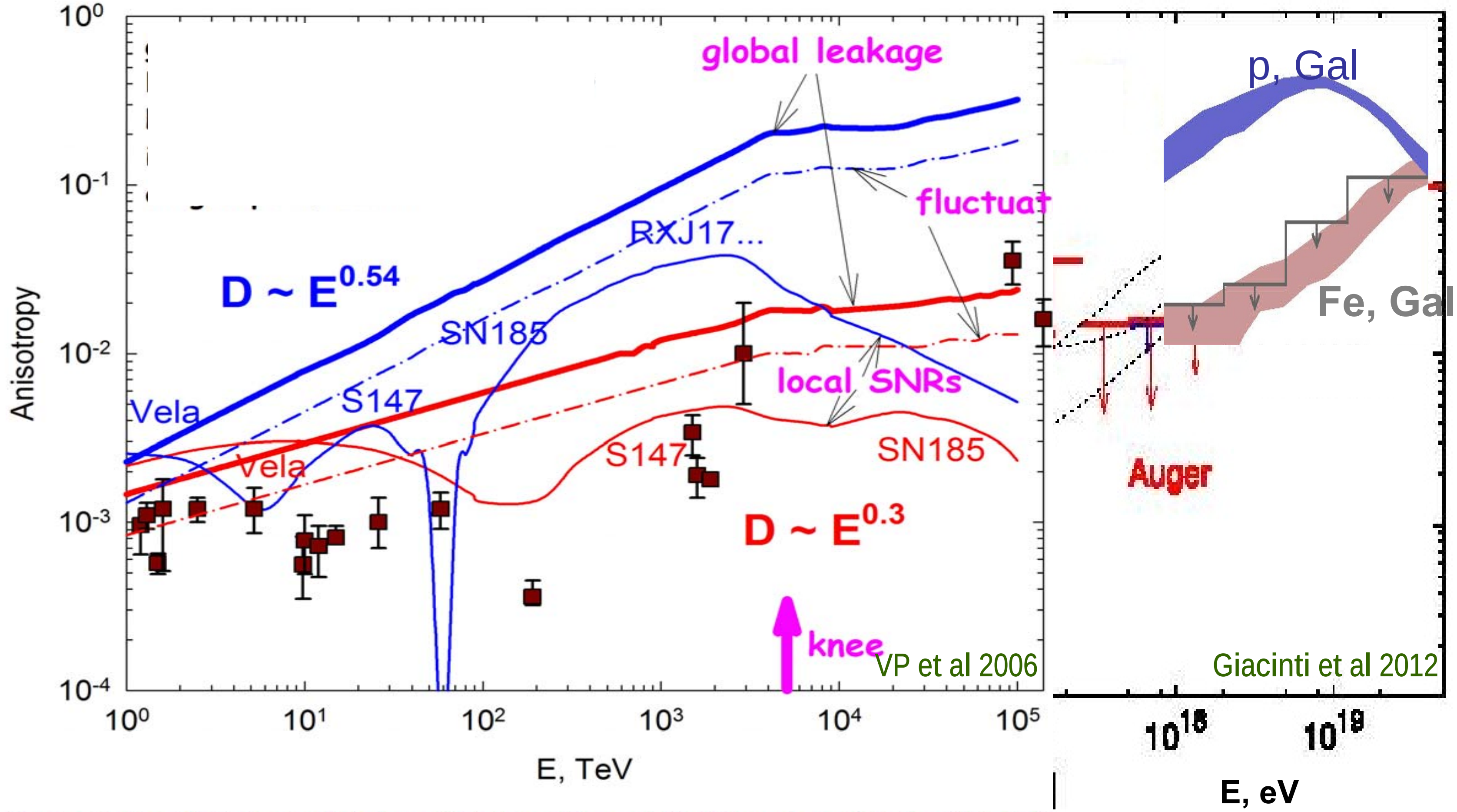

Gomboshi et al. 1975, Linsley & Watson 1977, Lloyd-Evans 1982, Kifune et al. 1986, Lee & Ng 1987
Bird et al. 1989, Nagashima et al. 1989, Andreev et al. 1991, Cutler & Groom 1991, Fenton et al. 19
Mori et al. 1995, Aglietta et al. 1996, Efimov et al. 1997, Munakata et al. 1999, Ambrosio et al. 2003

transition to extragalactic component of cosmic rays

Greisen 1966, Zatsepin & Kuzmin 1966;
Gerasimova & Rozental 1961, Stecker 1969

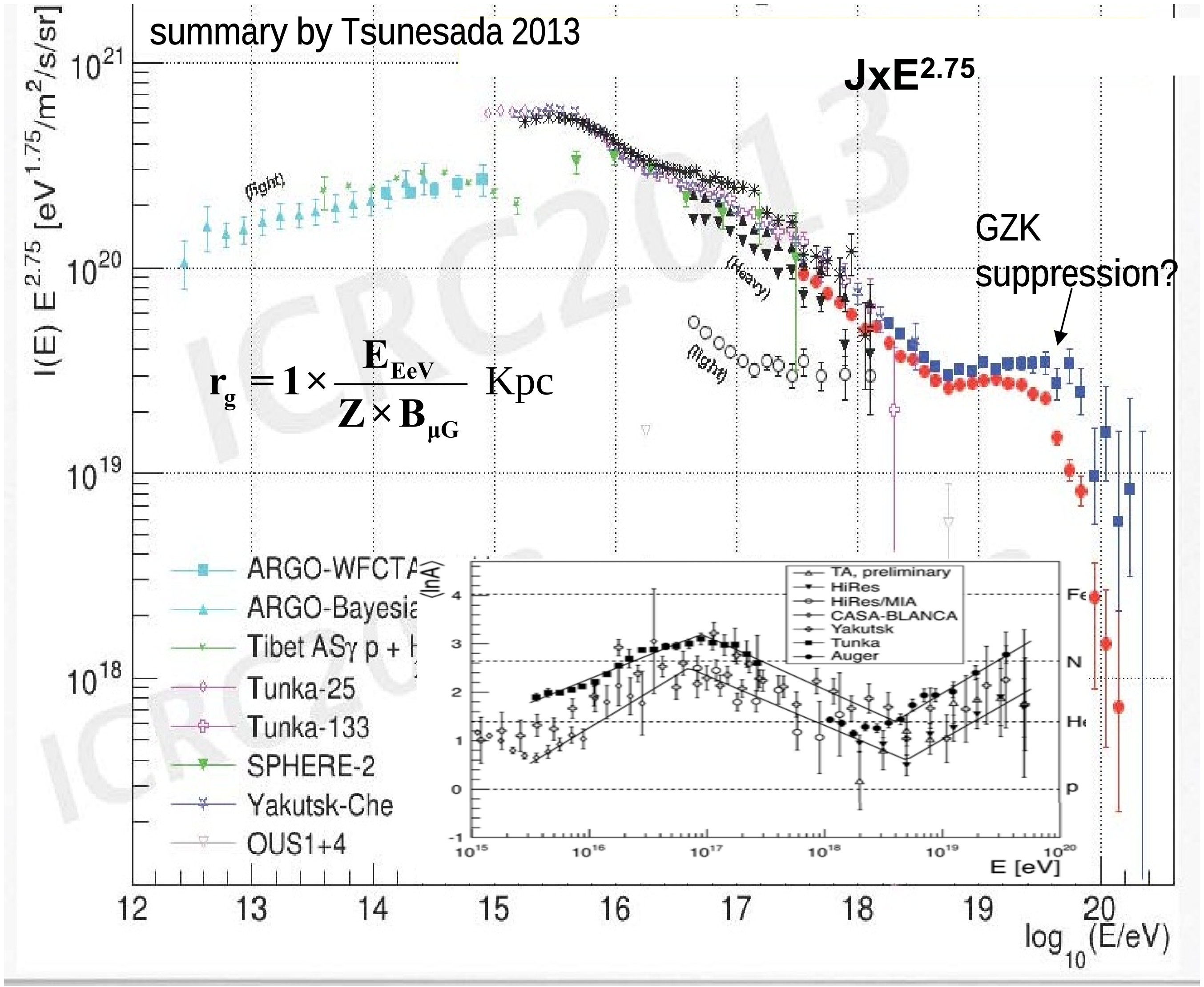

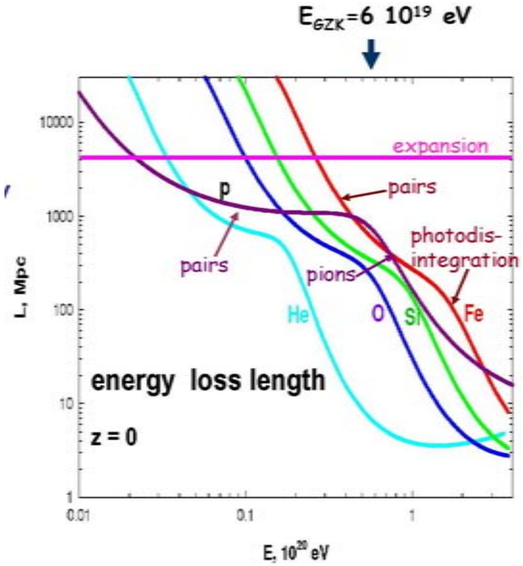

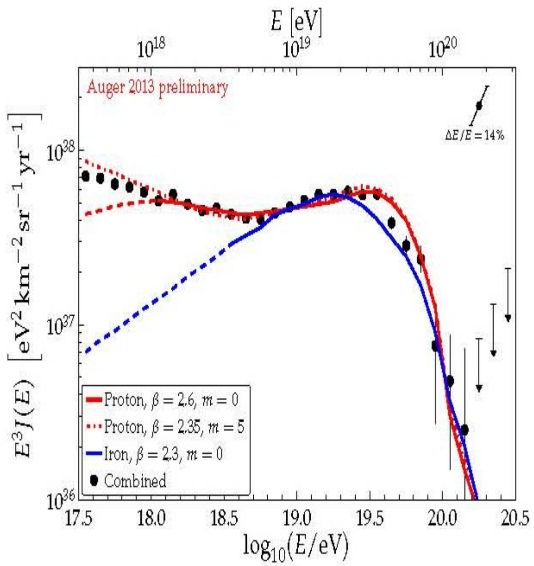

extragalactic sources of cosmic rays

energy release in units 10^{40} erg/(s Mpc^3)

needed in CR at $E > 10^{19.5}$ eV	SN	AGN jets	GRB	newly born fast pulsars (< 5ms)	accretion on galaxy clusters
$3\ 10^{-4}$ (Auger)	$3\ 10^{-1}$	3	$3\ 10^{-4}$	10^{-3}	10
	kin.	& $6\ 10^{-2}$ for	X/gamma	rotation	strong shocks
$8\ 10^{-3}$ for $E>10^9$ eV		$L_{kin} > 10^{44}$ erg/s			

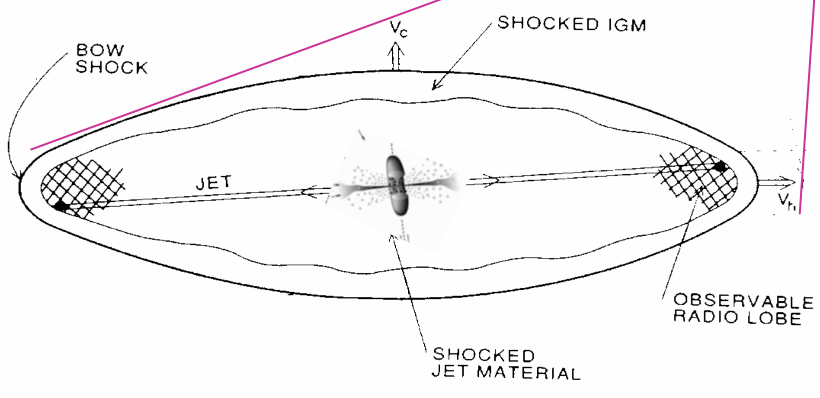

Schematic diagram of overpressured cocoons around jets (Begelman & Cioffi 1989).

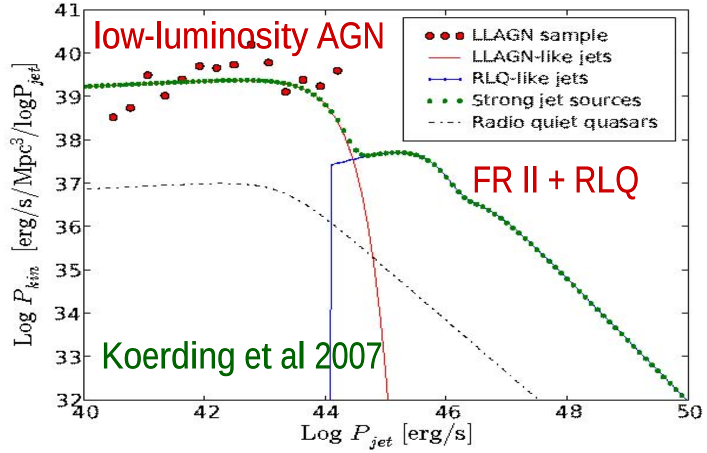

AGN jets

$$E_{max} \approx 10^{20} \times Z \times \beta^{1/2} \times \left(L_{jet} / 10^{45}\ erg/s \right)^{1/2}\ eV$$

Lovelace 1976, Biermann & Strittmatter 1987, Norman et al 1995, Lemoine & Waxman 2009

fast new born pulsars
$B = 10^{12} \ldots 10^{13}$ G

$$E_{max} \approx 10^{19} \times Z \times \left(\Omega / 10^4 sec \right)^2\ eV$$

Gunn & Ostriker 1969, Berezinsky et al. 1990, Arons 2003, Blasi et al 2000, Fang et al. 2013

Auger

- transition to heavy elements above 10^{19} eV

- anisotropy

TA+HiRes

- proton dominated composition

- "hot spot" anisotropy

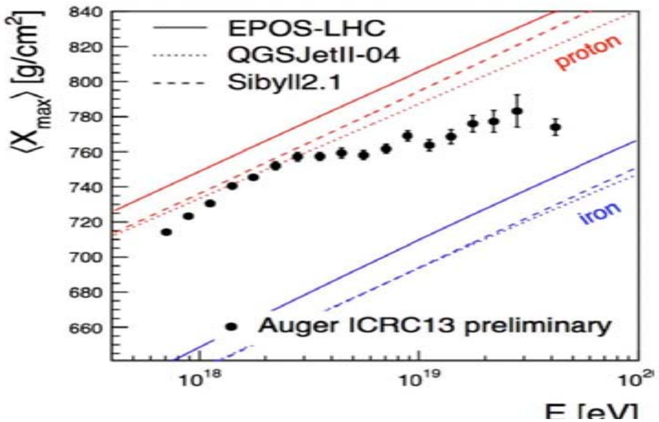

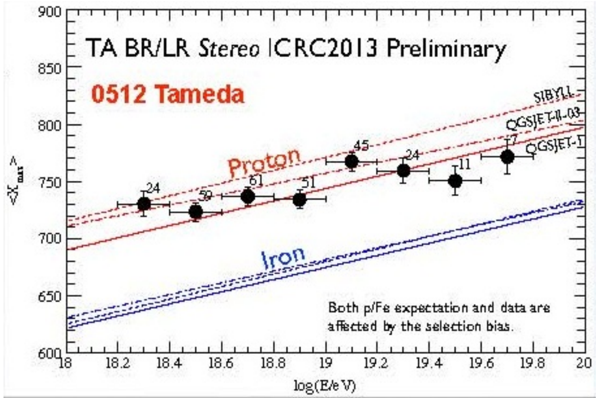

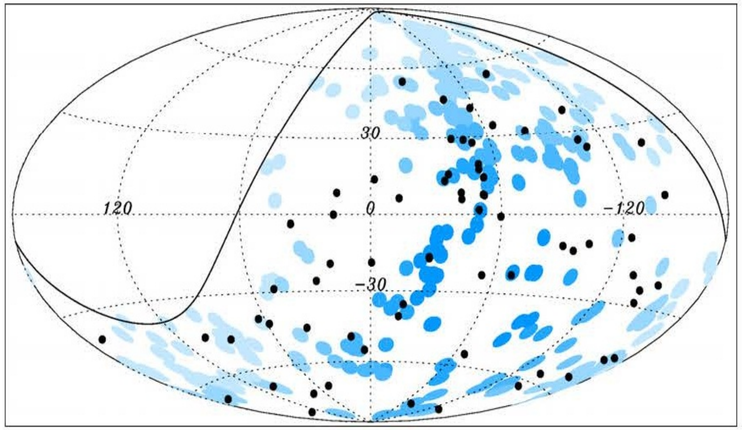

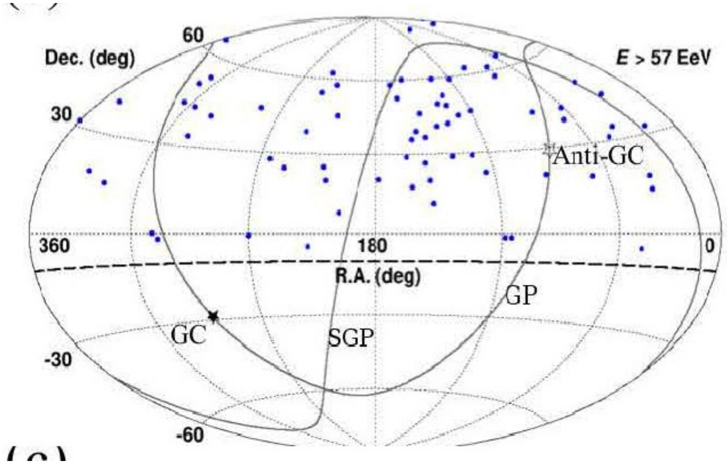

for heavy composition: $\mathbf{E_{max}/Z = 4 \times 10^{18}}$ **eV** easier to accelerate cosmic rays but difficult to identify their sources; production of neutrinos is suppressed (Berezinsky - "disappointing" model)

very high energy neutrinos of cosmic origin

IceCube neutrino detector

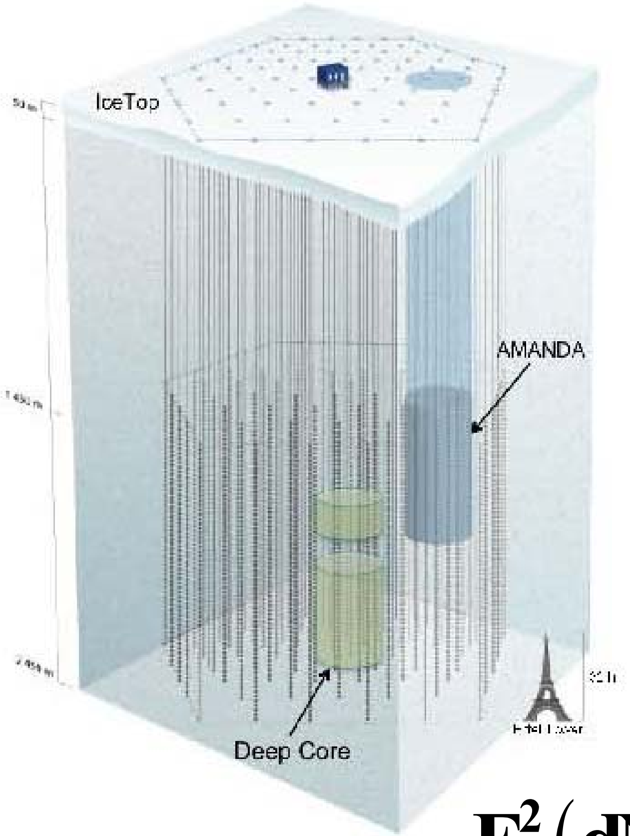

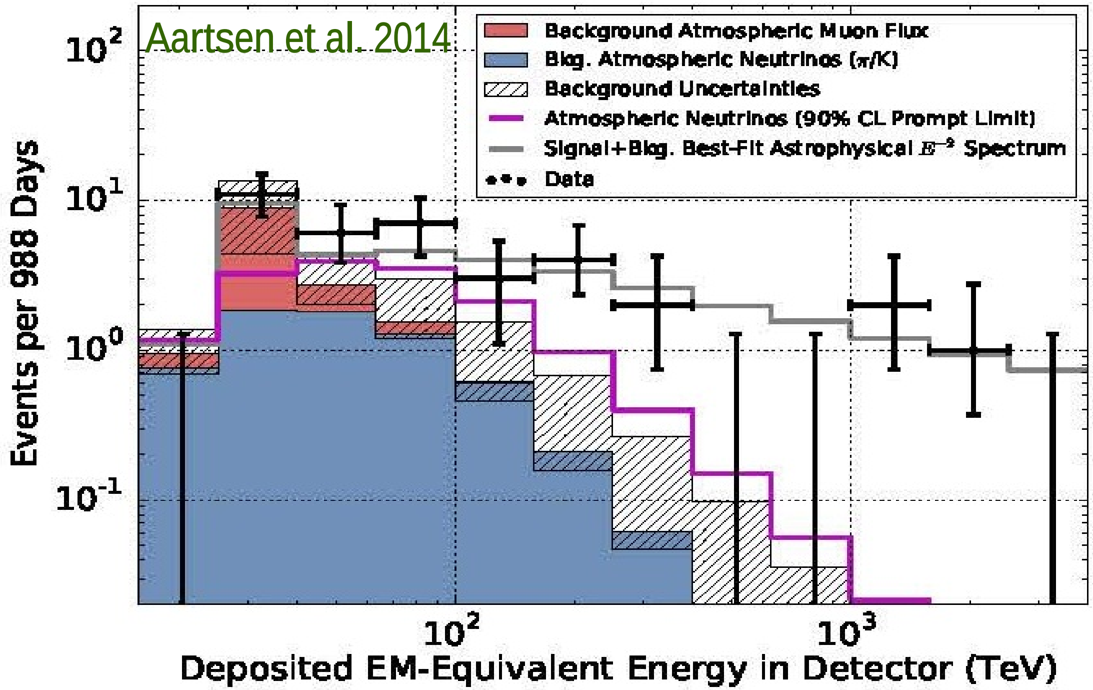

100 TeV 1000 TeV

$$E_\nu^2 \left(dN/dE_\nu \right) = (0.95 \pm 0.3) \times 10^{-8}\ \mathrm{GeV\,cm^{-2}\,s^{-1}\,sr^{-1}}$$

3-year data:
excess of 37 neutrinos above atmospheric background (>5.7 sigma) at 3.10^{13} to 2.10^{15} eV

- cosmic neutrino flux per flavor with possible suppression above 2 PeV;
- equal flavor ratio 1:1:1;
- isotropic sky distribution

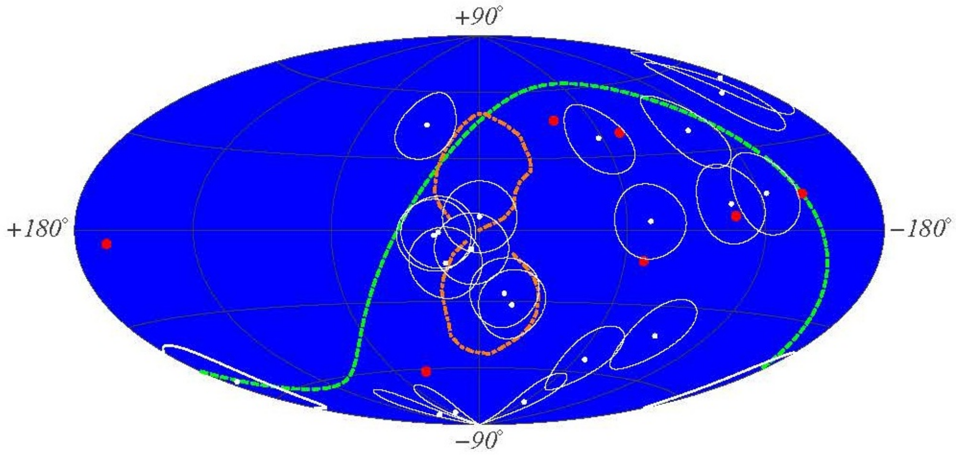

28 IceCube neutrino events in Galactic coordinates. The 21 shower-like events are shown with 15° error circles around the approximate positions (small white points) reported by the IceCube Collaboration. The 7 track-like events are shown as larger red points. Also shown are the boundaries of the Fermi bubbles (dot-dashed line) and the Equatorial plane (dashed line). Razzaque 2013

neutrino production
in cosmos is possible via
interactions $p\gamma, pp(n)$
and decay chains

$$\pi^+ \to \mu^+ \nu_\mu,\ \mu^+ \to e^+ \nu_e \bar{\nu}_\mu$$

plus neutrino oscillations

- Galactic sources may account only for a minority of events
- cosmogenic (GZK) neutrino production is inefficient
- can be produced in extragalactic sources of UHE cosmic rays; not in GRB

WB bound? Waxman & Bahcall 1999

Conclusions

Cosmic ray origin scenario where supernova remnants serve as principle accelerators of cosmic rays in the Galaxy is strongly confirmed by recent numerical simulations.

Accurate data on cosmic rays in the energy range 10^{17} to 10^{19} eV, where the transition from Galactic to extragalactic component occurs are becoming available.

Eliminating the uncertainties with energy spectrum and composition is necessary for understanding of cosmic ray origin at the highest energies.